Palladium–Based Plasmonic Perfect Absorber in the Visible Wavelength Range and Its Application to Hydrogen Sensing

6 AUTHORS, INCLUDING:

Andreas Tittl

École Polytechnique Fédérale de Lausanne

22 PUBLICATIONS **199** CITATIONS

Palladium-Based Plasmonic Perfect Absorber in the Visible Wavelength Range and Its Application to Hydrogen Sensing

Andreas Tittl,[†] Patrick Mai,[†] Richard Taubert,[†] Daniel Dregely,[†] Na Liu,[‡] and Harald Giessen*[,†]

[†]4th Physics Institute and Research Center SCOPE, University of Stuttgart, D-70569 Stuttgart, Germany
[‡]Department of Electrical and Computer Engineering, Rice University, Houston, Texas 77005, United States

S *Supporting Information*

ABSTRACT: We report on the experimental realization of a palladium-based plasmonic perfect absorber at visible wavelengths and its application to hydrogen sensing. Our design exhibits a reflectance <0.5% and zero transmittance at 650 nm and the operation wavelength of the absorber can be tuned by varying its structural parameters. Exposure to hydrogen gas causes a rapid and reversible increase in reflectance on a time scale of seconds. This pronounced response introduces a novel optical hydrogen detection scheme with very high values of the relative intensity response.

KEYWORDS: Plasmonics, LSPR resonances, perfect absorbers, palladium, sensor, hydrogen sensing
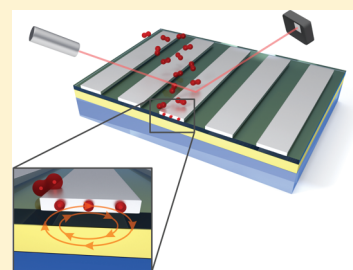
Subwavelength metallic nanostructures exhibit unique optical properties at visible wavelengths which are dominated by localized surface plasmon resonances.[1] Their resonance energy strongly depends on the shape, size, and material properties of the nanoparticles as well as on the dielectric function of the surrounding medium. Complex coupled plasmonic systems show intriguing phenomena such as hybridization,[2,3] electromagnetically induced transparency,[4] and Fano resonances.[5,6] Additionally, the strong local field enhancement at the metallic surfaces enables several applications in the fields of, i.e., nonlinear optics,[7] plasmon-enhanced photovoltaics,[8] and most importantly chemical and biological sensing.[9,10]

Recently, plasmonic structures with large (or "perfect") absorption in a certain wavelength range have attracted considerable interest.[11−15] So far near perfect absorption has been realized experimentally in the gigahertz to terahertz range[11,12] as well as in the near-infrared region.[13,14] A design in the visible region based on a subwavelength hole array has so far only been studied theoretically.[15]

In this Letter we present a simple multilayer sample design based on palladium nanowires which exhibits near-perfect absorption at visible wavelengths. We then introduce a new plasmonic hydrogen detection scheme which uses this concept to improve the performance of nanoplasmonic gas sensors due to our background-free detection scheme.[13]

We choose palladium because of the strong change of its optical properties upon hydrogen absorption. Due to hydrogen incorporation palladium undergoes a phase transition from a metal to a metal hydride which leads to an expansion of the palladium lattice.[16] Additionally, the incorporation leads to a shift of the Fermi level of the conduction electrons[17] and therefore significantly changes the real and imaginary part of the dielectric function of palladium. Many hydrogen detection schemes based on this effect have already been proposed.[18]

Optical detection is of particular interest since hydrogen forms an explosive atmosphere when it mixes with air at volume concentrations ranging from 4% to 76%. All-optical sensors minimize the risk of explosion and therefore are highly desirable for industrial and automotive applications.

Early optical sensing schemes were based on the measurement of optical switching in thin palladium films due to hydrogen incorporation.[19] Recently, several new types of hydrogen sensors based on nanoplasmonic effects have been proposed.[16,20,21] In contrast to traditional plasmonic refractive index sensors, novel plasmonic sensing concepts utilize a hydrogen-induced frequency shift of the plasmon oscillations excited in palladium nanostructures.

In our perfect absorber structure we utilize the plasmonic response of palladium nanowires stacked above a 200 nm thick gold film. The two layers are separated by a 65 nm dielectric MgF_2 spacer layer as depicted in Figure 1a.

When light polarized perpendicular to the wires impinges on our structure, localized plasmon oscillations are excited in the palladium wires. The resulting charge distribution leads to the antiphase oscillation of a mirror plasmon in the thick gold film below, giving rise to a circular current distribution and consequently a magnetic response of our structure.[13] This leads to efficient coupling of the incident light into the structure where it is dissipated as heat in the metallic components and (for nonzero absorptivity) the dielectric spacer layer.

In a simple model the structure can be described as an effective medium with complex electric permittivity $\varepsilon(\lambda)$ and magnetic permeability $\mu(\lambda)$. By carefully choosing the geometric parameters of the structure, both ε and μ can be adjusted such that its
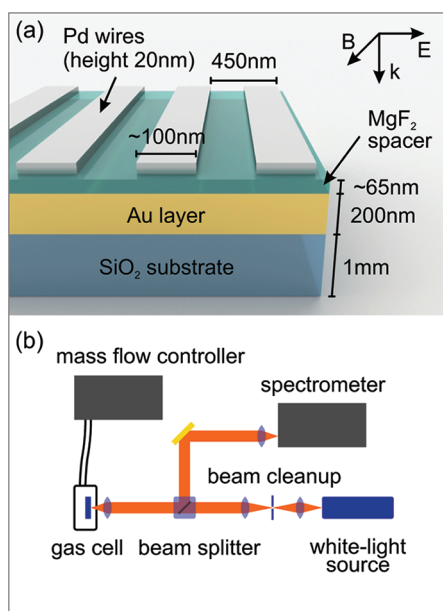
Figure 1. (a) A side view of the sensor. Palladium nanowires are stacked above a gold mirror. The layers are separated by a MgF_2 film. (b) A sketch of the experimental setup including the mass-flow controllers used to set the desired hydrogen concentrations.

complex impedance $Z_{struc} = (\mu/\varepsilon)^{1/2}$ is matched to the vacuum impedance $Z_{vac} = 1$ (in cgs units) for a given wavelength λ_0. This impedance matching results in zero reflectance $R = (Z_{vac} - Z_{struc})/(Z_{vac} + Z_{struc})$. Since the transmission through the sample is completely suppressed by the Au film, an absorbance of $A = 1 - R - T = 1$ can be obtained.

Although the impedance matching picture using effective ε and μ is a phenomenological one in our case due to the large periodicity, it describes the appropriate design principles very well and aids in the design of future absorbers and sensors.

In order to examine the optical properties of our structure, we perform numerical calculations based on a scattering matrix approach.[22] The dielectric functions ε of palladium and gold are taken from tabulated data reported by Vargas et al.[23] and Johnson and Christy,[24] respectively. For the MgF_2 spacer layer, $\varepsilon = 1.97$ is assumed.

To obtain a cohesive picture of our design's absorptive characteristics, we compute reflectance spectra for a multitude of parameter combinations of the crucial geometric parameters wire width and spacer height. Wire height and periodicity are fixed at 20 and 450 nm, respectively. We then extract the lowest reflectance value as well as its spectral location from the resulting data. Figure 2a shows a color-coded plot of the lowest reflectance for every point of the parameter space. A region of minimal reflectance can be seen for wire widths around 100 nm and spacer heights around 60 nm.

Absorption remains >99% for a fixed spacer height in this parameter range whereas the spectral location of the reflectance dip can be tuned from 630 to 820 nm by changing the wire width from 90 to 130 nm as shown in Figure 2b. The minimum reflectance diagram also identifies regions that are not very sensitive to spacer height variations, which aids reliable fabrication.

The perfect absorber can be utilized as a sensor since hydrogen-induced changes of ε in the palladium wires result in an increased impedance mismatch and consequently in a reduction of the perfect absorption.
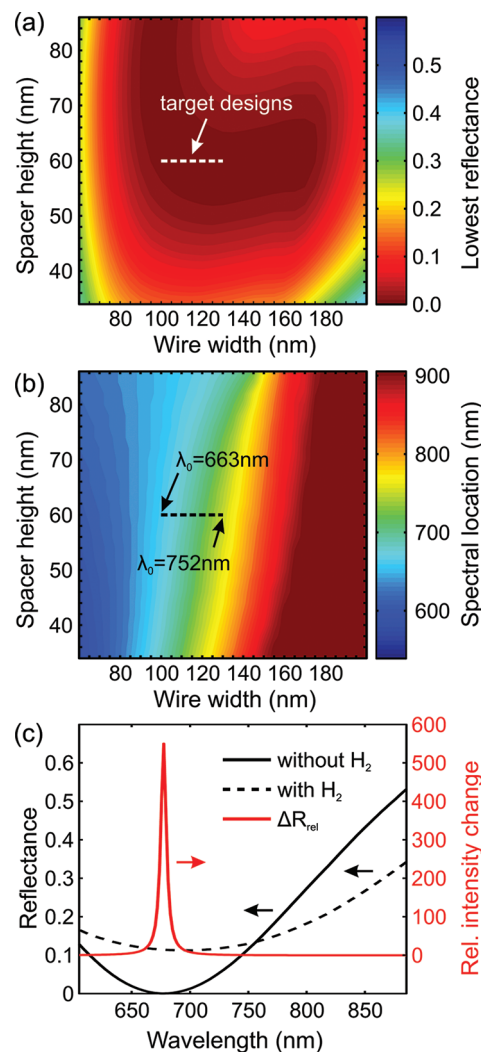

Figure 2. (a) Simulated lowest reflectance for different values of the structure parameters wire width and spacer height. A large number of value pairs suitable for utilization in a perfect absorber geometry can be identified next to the dashed line. (b) Simulated spectral location of the reflectance minimum. The spectral location of the perfect absorption can easily be controlled by varying the wire width. (c) Simulated response of the sensor structure to hydrogen exposure. High values of $\Delta R_{rel} = (R_{H_2} - R_0)/R_0$ can be achieved close to the spectral location of perfect absorption.

To investigate the response of one of the target structures to hydrogen exposure, we calculate reflectance spectra for palladium wires with a hydrogen content of 0% and 82%.[23] The results together with the relative intensity change $\Delta R_{rel} = (R_{H_2} - R_0)/R_0$ are shown in Figure 2c. Since the reflectivity at λ_0 is $R \approx 0$, very high ΔR_{rel} values of more than 500 can be achieved. This shows that our plasmonic structure offers a very large potential for hydrogen sensing.

It is important to note that our structure does not offer a completely angle-independent optical response. The reasons are the periodicity of 450 nm and the associated Rayleigh anomaly. However, since our sensor is designed to operate only at normal incidence, angle independence is not required in our case. Nevertheless, in the supplement we present a nearly angle-independent absorber design (periodicity 300 nm, Pd wire width 100 nm, wire thickness 30 nm, Al_2O_3 spacer height 35 nm, Au
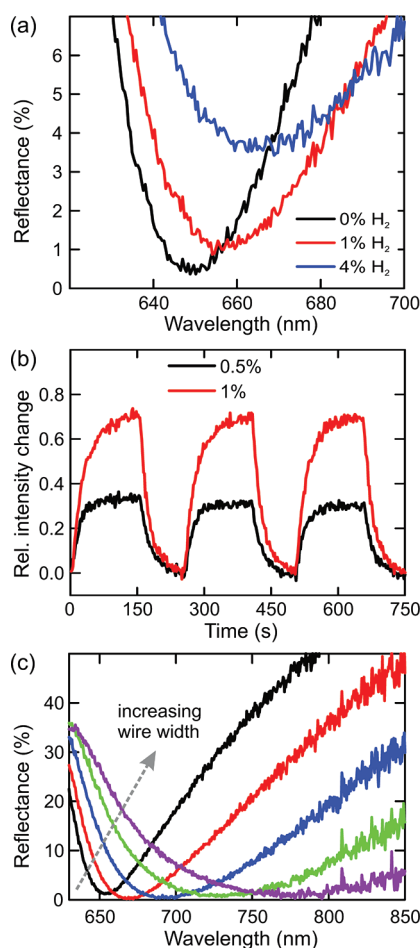
Figure 3. (a) Reflectance of the absorber for different hydrogen concentrations. Our sensor exhibits near-perfect absorption at 650 nm and hydrogen incorporation leads to a pronounced change of the reflectance spectrum. (b) The relative change of reflected intensity measured over time at the wavelength of perfect absorption λ_0. Three cycles of hydrogen exposure for two different concentrations are shown. (c) Reflectance spectra for absorber samples with different wire widths and constant spacer height. The use of palladium is also optically advantageous, since its large losses lead to a rather broad band perfect absorber response.

mirror height 200 nm) together with reflectance measurements, yielding up to 95% absorbance.

We fabricated the samples under investigation in a multistep process at cleanroom conditions. Starting from a clean substrate (Heraeus Infrasil) we subsequently deposited films of 200 nm of gold and 65 nm of MgF$_2$ at a pressure of 10^{-6} mbar using thermal evaporation. The spacer layer thickness of 65 nm was chosen to compensate for the material's granularity. Palladium gratings with different widths of the wires at a fixed grating period of 450 nm were fabricated using a standard electron-beam lithography lift-off technique. The structure area size of the single fields is 300 μm $\times$ 300 μm. After evaporation of 20 nm palladium the lift-off procedure was performed in the solvent NMP. Scanning electron micrographs were taken to determine the period and width of the wires. In principle, these structures might also be fabricated over areas as large as square decimeters using interference lithography.[25]

In order to optically characterize our perfect absorber, we measure the reflectance of the sample in the visible wavelength

range. Collimated and linearly polarized white light from an arc source is focused to the single arrays using a microscope objective with NA 0.3. Light reflected from the sample is separated from the incident light via a 50/50 beamsplitter cube and detected as a function of wavelength using a commercial spectrometer (Acton Advanced SP 2500i) with an attached Peltier-cooled CCD camera (see Figure Figure 1b). As a reference we use the reflectance of a plain gold mirror.

Figure 3a shows a minimal reflectance of 0.5% at $\lambda_0 = 650$ nm and thus near-perfect absorption for a wire width of 100 nm. This is in excellent agreement with the simulated behavior of the structure.

The same sample is used for measuring time-resolved reflectance spectra in the presence of 0.5–4.0% H$_2$ in a N$_2$ carrier gas at room temperature and atmospheric pressure (see Figure 3a).

For the 4.0% H$_2$ concentration, which is the explosion threshold, we detect a maximum spectral shift of 19 nm and an increase of the reflectance at λ_0 from 0.5% to 4.9%. Due to the low values of the reflectance at resonance, we obtain a large relative change of reflectivity $\Delta R_{rel} = (R_{H_2} - R_0)/R_0$ of 8.8. Compared to conventional thin film palladium hydrogen sensors[26] we can increase ΔR_{rel} by 1 order of magnitude. To further characterize the sensor, we measure the temporal response at a fixed wavelength of $\lambda_0 = 650$ nm during three sensor cycles where the hydrogen concentration was repeatedly changed from 0% to 4% as depicted in Figure 3b. We are able to detect hydrogen concentrations down to 0.5% reliably and reproducibly.

The response time of our sensor is in the range of 10–50 s. It can be reduced by utilizing different materials for the plasmonic wires such as palladium/nickel alloys.[26] Since the incorporation of hydrogen into the palladium lattice is a bulk effect,[27] designs with thinner wires could also improve the response time.

To demonstrate the spectral tunability of the reflectance dip, we examine samples with different widths of the palladium wires at a constant spacer height of 65 nm. For all samples we observe a reflectance <5% upon increasing the wire width from 90 to 130 nm. This results in a red shift of the reflection dip (see Figure 3c). Since for a fixed spacer height perfect impedance matching cannot be obtained for different wire widths, the modulation depth of the reflectance has a maximum for $w = 100$ nm and decreases with higher or lower widths. We can also observe an increase of the line width of the dip for higher wire widths.

In conclusion, we have experimentally demonstrated that near-perfect absorption at visible wavelengths can be obtained using a simple design based on plasmonic palladium nanowires in combination with a dielectric spacer layer and a gold mirror. Our structure shows a reflectance of 0.5% which in combination with a complete suppression of transmission yields an absorbance of $A \approx 99.5\%$. The spectral location of maximum absorbance can be tuned over a range of approximately 100 nm by varying the width of the palladium wires.

We utilized our Pd perfect absorber structure for hydrogen sensing and were able to reliably detect concentrations down to 0.5% H$_2$ in air with response times in the range of seconds. Optimizing sample fabrication and measurements even further, this already pronounced response should enable extremely sensitive optical gas detection schemes down to the parts per million range in the future.

■ ASSOCIATED CONTENT

ⓢ Supporting Information. Design and reflectance measurements of a palladium-based plasmonic perfect absorber

optimized for greater angle-independence. This material is available free of charge via the Internet at http://pubs.acs.org.

■ AUTHOR INFORMATION

Corresponding Author
*E-mail: giessen@physik.uni-stuttgart.de.

■ REFERENCES

(1) Halas, N. J. *Nano Lett.* **2010**, *10*, 3816–3822.

(2) Nordlander, P.; Oubre, C.; Prodan, E.; Li, K.; Stockman, M. I. *Nano Lett.* **2004**, *4*, 899–903.

(3) Halas, N. J.; Lal, S.; Chang, W.-S.; Link, S.; Nordlander, P. *Chem. Rev.* **2011**, *111*, 3913–61.

(4) Liu, N.; Langguth, L.; Weiss, T.; Kästel, J.; Fleischhauer, M.; Pfau, T.; Giessen, H. *Nat. Mater.* **2009**, *8*, 758–762.

(5) Hentschel, M.; Saliba, M.; Vogelgesang, R.; Giessen, H.; Alivisatos, A.; Liu, N. *Nano Lett.* **2010**, *10*, 2721–6.

(6) Luk'yanchuk, B.; Zheludev, N. I.; Maier, S. A.; Halas, N. J.; Nordlander, P.; Giessen, H.; Chong, C. T. *Nat. Mater.* **2010**, *9*, 707–15.

(7) Klein, M. W.; Enkrich, C.; Wegener, M.; Linden, S. *Science* **2006**, *313*, 502–504.

(8) Atwater, H. A.; Polman, A. *Nat. Mater.* **2010**, *9*, 205–13.

(9) Anker, J. N.; Hall, W. P.; Lyandres, O.; Shah, N. C.; Zhao, J.; Van Duyne, R. P. *Nat. Mater.* **2008**, *7*, 442–453.

(10) Lal, S.; Link, S.; Halas, N. J. *Nat. Photonics* **2007**, *1*, 641–648.

(11) Landy, N. I.; Sajuyigbe, S.; Mock, J. J.; Smith, D. R.; Padilla, W. J. *Phys. Rev. Lett.* **2008**, *100*, 207402.

(12) Tao, H.; Bingham, C. M.; Strikwerda, A. C.; Pilon, D.; Shrekenhamer, D.; Landy, N. I.; Fan, K.; Zhang, X.; Padilla, W. J.; Averitt, R. D. *Phys. Rev. B* **2008**, *78*, 241103.

(13) Liu, N.; Mesch, M.; Weiss, T.; Hentschel, M.; Giessen, H. *Nano Lett.* **2010**, *10*, 2342.

(14) Hao, J.; Wang, J.; Liu, X.; Padilla, W. J.; Zhou, L.; Qiu, M. *Appl. Phys. Lett.* **2010**, *96*, 251104.

(15) Hu, C.; Zhao, Z.; Chen, X.; Luo, X. *Opt. Express* **2009**, *17*, 11039–11044.

(16) Langhammer, C.; Zori, I.; Kasemo, B. *Nano Lett.* **2007**, *7*, 3122–3127.

(17) Kishore, S.; Nelson, J.; Adair, J.; Eklund, P. *J. Alloys Compd.* **2005**, *389*, 234–242.

(18) Favier, F. *Science* **2001**, *293*, 2227–2231.

(19) Chtanov, A.; Gal, M. *Sens. Actuators, B* **2001**, *79*, 196–199.

(20) Maeda, E.; Mikuriya, S.; Endo, K.; Yamada, I.; Suda, A. *Appl. Phys. Lett.* **2009**, *95*, 133504.

(21) Liu, N.; Tang, M. L.; Hentschel, M.; Giessen, H.; Alivisatos, A. P. *Nat. Mater.* **2011**, *10*, 631–636.

(22) Weiss, T.; Gippius, N. A.; Tikhodeev, S. G.; Granet, G.; Giessen, H. *J. Opt. A: Pure Appl. Opt.* **2009**, *11*, 114019.

(23) Vargas, W. E.; Rojas, I.; Azofeifa, D. E.; Clark, N. *Thin Solid Films* **2006**, *496*, 189–196.

(24) Johnson, P. B.; Christy, R. W. *Phys. Rev. B* **1972**, *6*, 4370–4379.

(25) Guo, H. C.; Nau, D.; Radke, A.; Zhang, X. P.; Stodolka, J.; Yang, X. L.; Tikhodeev, S. G.; Gippius, N. A.; Giessen, H. *Appl. Phys. B: Laser Opt.* **2005**, *81*, 271.

(26) Fedtke, P.; Wienecke, M.; Bunescu, M.; Pietrzak, M.; Deistung, K.; Borchardt, E. *Sens. Actuators, B* **2004**, *100*, 151–157.

(27) Flanagan, T. *Annu. Rev. Mater. Sci.* **1991**, *21*, 269–304.

■ NOTE ADDED AFTER ASAP PUBLICATION

This article was published ASAP on September 7, 2011. Figure 2 has been updated. The corrected version was posted on September 28, 2011.